AD_____

Award Number: W81XWH-11-1-0299

TITLE: Non-invasive MR-guided HIFU Therapy of TSC-Associated Renal Angiomyolipomas

PRINCIPAL INVESTIGATOR: Yu Li

CONTRACTING ORGANIZATION: Cincinnati Children's Hospital Medical Center
Cincinnati, OH 45229-3026

REPORT DATE: July 2013

TYPE OF REPORT: Annual

PREPARED FOR: U.S. Army Medical Research and Materiel Command
Fort Detrick, Maryland 21702-5012

DISTRIBUTION STATEMENT: Approved for Public Release;
Distribution Unlimited

REPORT DOCUMENTATION PAGE

Form Approved
OMB No. 0704-0188

1. REPORT DATE	2. REPORT TYPE	3. DATES COVERED
July 2013	Annual	1 July 2012 – 30 June 2013

4. TITLE AND SUBTITLE

Non-invasive MR-guided HIFU Therapy of TSC-Associated Renal Angiomyolipomas

5a. CONTRACT NUMBER

5b. GRANT NUMBER
W81XWH-11-1-0299

5c. PROGRAM ELEMENT NUMBER

6. AUTHOR(S)

Yu Li

E-Mail: Yu.Li@cchmc.org

5d. PROJECT NUMBER

5e. TASK NUMBER

5f. WORK UNIT NUMBER

7. PERFORMING ORGANIZATION NAME(S) AND ADDRESS(ES)

Cincinnati Children's Hospital Medical Center
Cincinnati, OH 45229-3026

8. PERFORMING ORGANIZATION REPORT NUMBER

9. SPONSORING / MONITORING AGENCY NAME(S) AND ADDRESS(ES)
U.S. Army Medical Research and Materiel Command
Fort Detrick, Maryland 21702-5012

10. SPONSOR/MONITOR'S ACRONYM(S)

11. SPONSOR/MONITOR'S REPORT NUMBER(S)

12. DISTRIBUTION / AVAILABILITY STATEMENT
Approved for Public Release; Distribution Unlimited

13. SUPPLEMENTARY NOTES

14. ABSTRACT

This report is a summary of our first year's work on the proposed research. During this period, our effort was focused on technological development for thermal ablation in mice. Our goal was to establish a small-animal MR-guided HIFU experimental system that enables simultaneous HIFU ablation and MR guidance. This goal was achieved and our experimental results demonstrated the basic function of the experimental system in in-vitro studies. We have laid the groundwork for the feasibility investigation of mouse tumor ablation in the second year. Based on the current progress, we will continue work on our technological improvement of MR-guided HIFU system for in-vivo studies. We believe this system will be ready for animal experiments after several further in-vitro studies in two or three months.

15. SUBJECT TERMS
MR-guided HIFU, renal angiomyolipoma, tumor, ablation, thermal therapy, TSC

16. SECURITY CLASSIFICATION OF:			17. LIMITATION OF ABSTRACT	18. NUMBER OF PAGES	19a. NAME OF RESPONSIBLE PERSON
a. REPORT	b. ABSTRACT	c. THIS PAGE			USAMRMC
U	U	U	UU	18	19b. TELEPHONE NUMBER *(include area code)*

Table of Contents

Page

Introduction

The long-term goal of this research is to develop a non-invasive technique for clinical management of TSC-associated renal angiomyolipomas. TSC is a genetic tumor predisposition syndrome characterized by the growth of lesions in multiple organ systems. Approximately 80% of TSC patients develop renal angiomyolipomas, a type of lesion composed of variable amounts of fat, smooth muscle, and vascular tissue. Renal angiomyolipomas are often benign and present with multiple lesions in each kidney. Patients with renal angiomyolipomas may experience discomfort, flank pain, hydronephrosis, hematuria, and hypertension. These lesions can also lead to acute hemorrhaging or chronic loss of renal function. In this research, we will use High Intensity Focused Ultrasound (HIFU) to ablate tumors and magnetic resonance (MR) imaging to monitor ablation. MR-guided HIFU enables “surgical procedures” to be performed deep within the body without incisions or punctures, providing a risk-free therapeutic approach to managing benign or malignant lesions.

The proposed project aims to investigate whether MR-guided HIFU offers the ability to ablate renal angiomyolipomas in a mouse tumor model. We expect that the research experience gained from this pre-clinical study will benefit our future study on non-invasive thermal therapy of renal angiomyolipomas in human with MR-guided HIFU. In the proposed work, we had planned to focus on the development of an MR-guided HIFU experimental system for thermal ablation in mouse kidneys in the first year and perform animal experiments using the technique developed in the second year.

The physical mechanisms underlying HIFU is that a HIFU transducer constructed with a concave shape and/or multiple elements has the ability to focus acoustic energy into a target volume having a diameter of a few millimeters. The focused acoustic energy induces a rapid rise in temperature (e.g. 70°C to 100°C), resulting in thermal necrosis of tissues in the target volume. Although HIFU offers the capability of thermal ablation, non-invasive thermal therapy is possible only if the focal spot of HIFU can be controlled within the body using the feedback information provided by medical imaging guidance. MR is superior to other imaging modalities because it provides both excellent soft-tissue visualization and the ability to monitor thermal delivery (temperature mapping). However, an intrinsic drawback of MR is the slow data acquisition speed limited by long relaxation time. As a result, we had expected to meet challenges in imaging mouse kidneys with respiratory movement.

Our first year's work led to the development of a small animal HIFU system with feedback control. In several in-vitro studies without motion concerns, we have demonstrated that the developed HIFU system offers the ability to focus acoustic energy within a small spot in a diameter of a few millimeters. During the second year, we proceeded with *in-vivo* studies and found that motion may be destructive to HIFU thermal treatment. Although parallel imaging has been proposed and used to address this issue in this work, it was found that the performance of parallel imaging is not satisfactory because coil array configuration is limited by small mouse anatomy. This challenge has delayed our animal experiment and we are actively seeking a different solution to resolving the problem. The proposed project has been extended until 2014 and a different research plan will be used to advance our research.

This report is a summary of our second year's work on the proposed research. The summary will focus on the technical challenges we met and provide details about why this challenge cannot be overcome using the proposed techniques. In addition, we will propose our alternative plan to conduct the proposed animal experiments in the third year. In this plan, two methods will be used to overcome the technical challenge we found in the second year's work.

Body

In the second year, our effort was focused on the proposed Task 3. We found that the proposed parallel imaging approach could not meet the requirements for feedback control in *in-vivo* studies due to the limitation posed by small-animal anatomy and acoustic power transmission.

Proposed Task 3: Optimization of the MR-guided HIFU system for thermal ablation of renal angiomyolipomas in a mouse orthotopic xenograft model (Stage 2: Months 13-18).
The real-time MR guidance of renal targets will be optimized in a free-breathing mouse orthotopic xenograft model developed in Task 2. The adaptive control system will be optimized for maximizing the effectiveness and safety of HIFU thermal ablation. 10 mice will be used. This *in-vivo* test is the preparation phase for the following systematic evaluation of MR-guided HIFU therapy in task 4.

Research accomplishment: Figure 1 shows the experimental system we developed for thermal ablation in phantoms and animals during the first year of this project. This setup allows the HIFU console to synchronize MRI scanning when running HIFU thermal ablation. The acoustic power delivery from the HIFU transducer can be dynamically updated by the HIFU console based on MRI information, providing a feedback control for the thermal delivery deep within the body. During second year, we used this system to investigate whether HIFU focal lesions may be formed deep inside the mouse body. In our initial attempts, healthy mice were used.

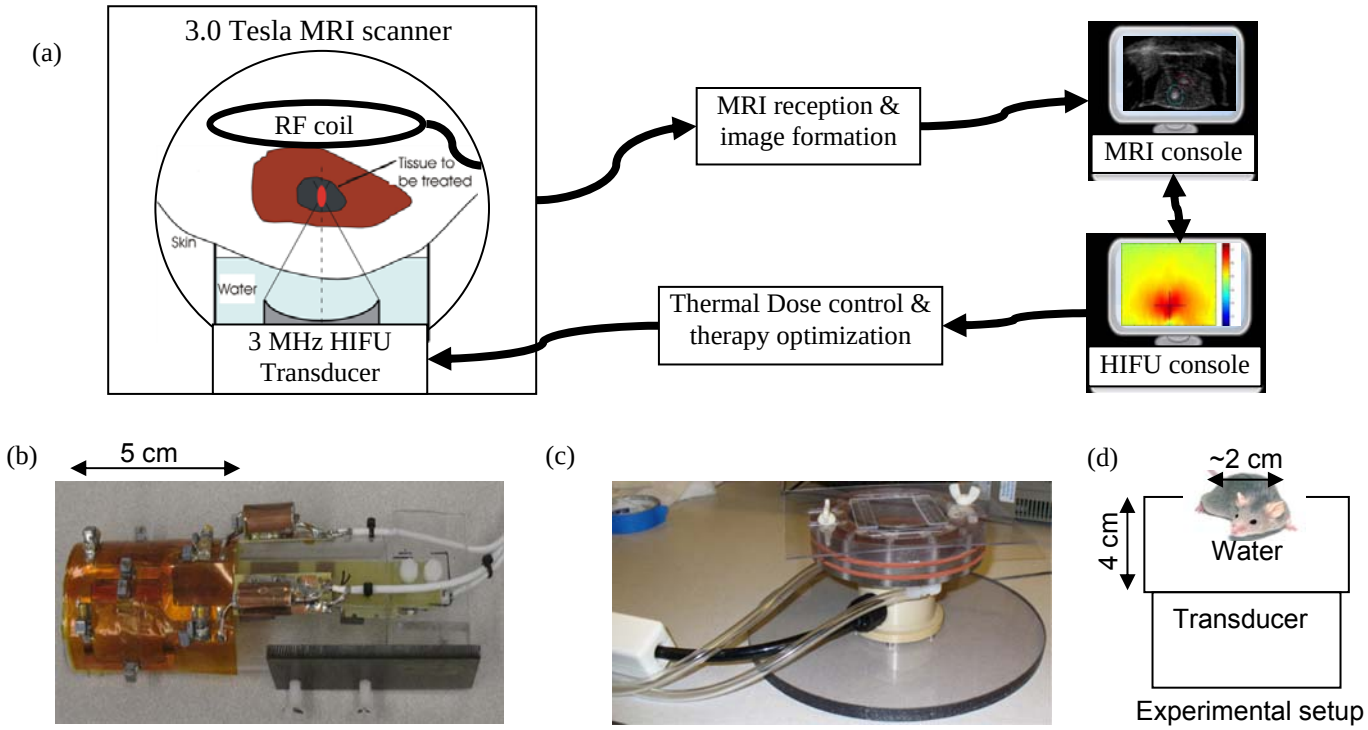

Figure 1. *A feedback control system for preclinical thermal therapy was established using MR-guided HIFU in the CCHMC IRC. The feedback control loop is formed using a 3.0 Tesla 32-channel Philips Achieva MR scanner (Philips HealthCare, Best, the Netherlands) and a Philips small-animal HIFU system (Philips HealthCare, Vantaa, Finland). This system uses an eight-channel 3 MHz sectored transducer (IMASONIC, Voray sur l'Ognon, France) for acoustic transmission. (a) Experimental setup. (b) An MRI coil was built for mouse imaging on Philips 3T scanner. (c) A mechanic stage was constructed for holding/stabilizing the mouse and the coil within the MRI scanner. Inside the stage, water will be used as the interface between the HIFU transducer and the animal.MRI console. (d) Placement of transducer and mouse inside the MRI scanner using the mechanic stage in (c).*

2a. Optimization of real-time MR guidance (Months 13-16).
Parallel imaging will be optimized to improve imaging speed and minimize motion artifacts in free-breathing mice. Specifically, the optimization will be performed to improve four major imaging methods, T_1 weighted

imaging, T_2 weighted imaging, stiffness weighted imaging, and phase imaging. It will be demonstrated that these imaging methods can provide accurate and real-time information about HIFU therapy delivery.

Research accomplishment: In this work, we found that the proposed parallel imaging technique cannot provide good performance due to coil array limitation. Figure 2 shows a HIFU ablation result using the experimental system (Figure 1) and a healthy animal. It was found that HIFU energy was successfully delivered into the animal body while temperature information was not able to be collected in real time using parallel imaging techniques. Our further investigation shows that the coil array we developed (Figure 1b) cannot provide good parallel imaging performance because the coil elements have to be larger than the mouse anatomy and positioned in a certain distance to the mouse. This configuration was practically limited by two factors: First, acoustic power transmission requires an open space to the abdominal region of the mouse. Since water has to be used to provide acoustic interface between the transducer and the mouse body, coil elements cannot be positioned close to the imaging target zone. Second, the coil elements have to large enough to achieve certain RF penetration due to the positioning limitation. As a result, spatial variation of multi-channel coil sensitivity was low, which significantly reduces the spatial encoding of coil sensitivity within the mouse body. Without sufficient imaging speed, dynamic imaging provides low image quality and temperature information (phase change of MR images) was distorted by imaging artifacts.

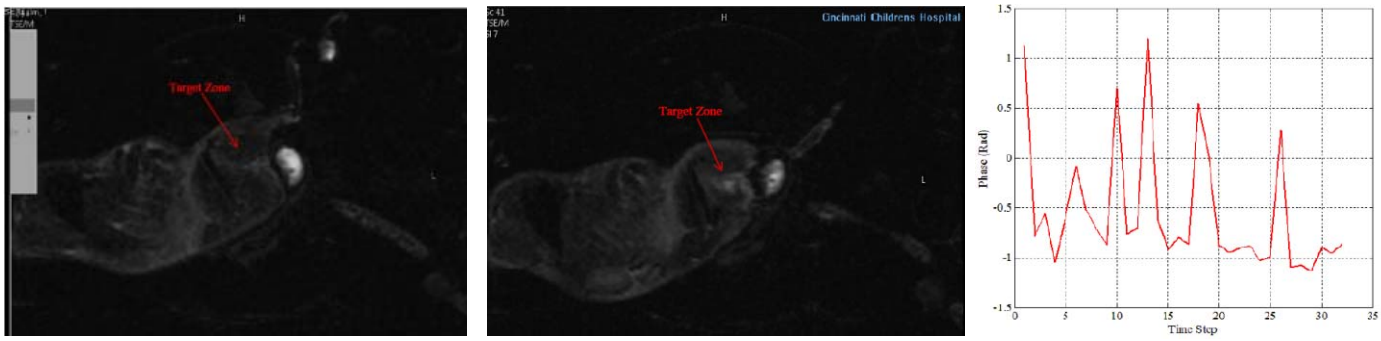

T1 image before ablation | T1 image after ablation | Temperature mapping

Figure 2. *Mouse HIFU ablation. Using the experimental system in Figure 1, HIFU ablation was performed in a healthy mouse. T1-weighted MR images were collected to determine whether a HIFU lesion was formed in the target zone. By comparing T1-weighted images before and after ablation, the contrast difference was found, implying HIFU lesion was produced deep inside the animal body. However, dynamic MR images were not able to provide accurate temperature information for real-time feedback control.*

2b. Optimization of the adaptive control system for HIFU (Months 17-18).
In free-breathing mice, the adaptive control system will be optimized to improve the localization and power of HIFU focal spot dynamically based on real-time MR guidance. It will be demonstrated that HIFU lesions can be effectively created irrespective of respiratory motion. The safety limit for thermal dose in HIFU ablation will also be determined. This safety limit will be used to determine the thermal dose for MR-guided HIFU therapy in the following task 4.

We have mathematically investigated the model for the implementation of adaptive control in HIFU treatment (See appendix 1). In this model, HIFU was considered as an inverse problem. Our collaborator developed a simulated model to test the possibility of adaptive control in real time. We are working on an approach to use the simulated model to predict HIFU treatment in mouse.

Alternative approaches to animal experiments: To overcome the challenge we found in the second year's work (Task 3), we have launched two efforts to seek a solution.

First, we developed research collaboration with Dr. Qiming Zhang's group in Pennsylvania State University. This group is working on a new type of Magnetoelectric Sensors for MR imaging. These sensors have the potential to provide imaging performance similar to RF coil array. However, their physical dimensions are in micro-meter (Figure 3) and they can be positioned as close to the mouse body as possible without interaction on HIFU acoustic transmission. In addition, since these sensors detect MR signals from sensing the mechanic

force generated by small magnetic field, no RF coupling is generated between different sensors. As a result, the channel number for MR imaging is unlimited. This is a significant advantage over conventional coil array technology. We are expecting to have the sensors ready for a test in January 2014. Once we have a set of sensors for our HIFU system, we will be able to continue our experiments.

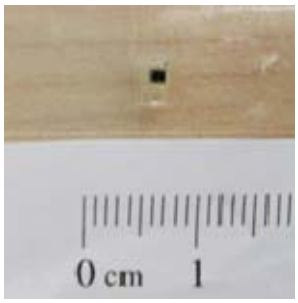

Figure 3. Magnetoelectric sensor we are developing for MR imaging.

Figure 4. Installment of 1.5 Tesla Philips Ingenia MR imaging system and human HIFU machine at the Cincinati Children's Hospital Medical Center.

Our second choice is to use the human HIFU system being installed at our institute. We purchased a 1.5 Tesla Ingenia MR imaging system with human HIFU from Philips HealthCare. Currently, the system was already delivered and is being installed in Imaging Research Center (Figure 4). This human HIFU system has 256 acoustic elements and offers the capability of moving the transducers in an arbitrary direction. More importantly, the commercial HIFU system allows the use of digital coil arrays provided by Ingenia system. As a result, we expect that this new system provides much better performance than the small animal HIFU system we are currently using. Once the system is ready, we planned to continue our animal experiments.

The final timeline of our animal experiments will be dependent on the progress of our two efforts described above. It is expected that further experiments on mouse will be conducted in January 2014.

Key Research Accomplishments

1. We found a technical challenge that arises from the coil array limitation posed by small animal anatomy and acoustic power transmission.
2. We launched two independent efforts to address the technical challenge met in the proposed Task 3.
    a. Magnetoelectric sensors are being developed through the research collaboration with Pennsylvania State University.
    b. A new human HIFU system is being installed. We are planning to transfer the animal experiments to this system.
3. A mathematical model was developed to investigate adaptive control algorithms in mouse HIFU ablation.

Reportable Outcomes

1. We have collaboratively developed a mathematical model with Dr. Donald French's group in the Mathematical Department at the University of Cincinnati (Appendix 1). This model provides a tool to investigate adaptive control problems in mouse HIFU treatment.
2. We have developed our collaboration Dr. Qiming Zhang's group. We are collaboratively developing a new type of magnetoelectric sensors that may be used to replace coil array in our current HIFU system for mouse ablation.

Conclusion

In summary, we have found new challenges in this project. From our preliminary investigation using *in-vivo* studies, we understood the physical mechanisms underlying the technical challenge and launched two independent efforts to address this technical challenge. We expect to continue our animal experiments at the beginning of 2014.

References

1. Z. Fang, F. Li, Q.M. Zhang, Magnetoelectric sensors with directly integrated charge sensitive readout circuit - Improved field sensitivity and signal-to-noise ratio, IEEE sensors 2010, 4875,.
2. D.A. French, D.A. Edwards, Perturbation approximation of solutions of a nonlinear inverse problem arising in olfaction experimentation, J. Math. Bio., 2007, *55*(5-6), 745-765.
3. J.M.J. Huttunen, T. Huttunen, M. Malinen, J.P. Kaipio, Determination of herterogeneous thermal parameters using ultrasound induced heating and MR thermal mapping, Phys. Med. Biol., 2006, 51, 1011-1032.

Appendix 1

See the following pages.

Working Draft:

Analysis of Inverse Problems arising in MRI assisted HIFU

Kristen Fox-Neff, Donald A. French and Benjamin Vaughan Jr.
Department of Mathematical Sciences, University of Cincinnati, Cincinnati, OH 45221-0025

Yu Li
Cincinnati Children's Hospital Medical Center, 3333 Burnet Avenue, Cincinnati, OH 45229.

November 25, 2012

1. Introduction:

High intensity focused ultrasound (HIFU) is applied to a region like the one in figure 1A which we label Ω and consists of tissue, skin, fat and blood in order to ablate cancerous tumors. Magnetic resonance imaging (MRI), figure 1B, is used to measure tissue temperatures and then estimate, with further mathematical modeling and scientific computing, various material parameters (e.g. conductivities, perfusions etc.) in the region and monitor the tumor remediation process. In this draft we study the mathematical model and various estimation procedures.

A. **B.**

Figure 1: Expermental apparatus and diagram for fMRI assisted HIFU analysis. **(A)** Example problem with Ultrasound transducer on the left and potential treatment region on the right. The diameter of the whole "liver" would be around 10 cm. **(B)** Magnetic resonance imaging machine (MRI).

Following [HHMK], we use the Helmholtz partial differential equation to model the pressure waves arising from the HIFU transducers;

$$\nabla \cdot \left(\frac{1}{\rho}\nabla p\right) + \frac{k^2}{\rho}p = 0 \qquad \text{in } \Omega. \tag{1}$$

Here $k = 2\pi f/c + i\alpha$, ρ is a positive density function, α is an absorption coefficient, c is sound speed and f

is a frequency. We append boundary conditions

$$\frac{\partial p}{\partial \nu} = i2\pi f \rho v_n \ \text{ on } \Gamma_U \quad \text{and} \quad \frac{\partial p}{\partial \nu} = 0 \ \text{ on } \partial\Omega - \Gamma_U. \tag{2}$$

The transducer velocity v_n is provided on boundary portion Γ_U. The temperature T in the liver/tumor which is induced by heating from the pressure waves is read by the MRI and evolves via

$$\rho C_T \frac{\partial T}{\partial t} = \nabla \cdot (\kappa \nabla T) - \beta(T - T_A) + Q \qquad \text{where } \beta = \omega_B C_B. \tag{3}$$

ω_B is blood flow rate; C_T & C_B are specific heat capacities of the tissue and blood, respectively. The $\beta(T - T_A)$ term models the averaged effects of blood vessels. Also, κ is a conductivity coefficient, T_A is an ambient temperature and $Q = \alpha|p|^2/(c\rho)$. Boundary and initial conditions for $T = T(x, t)$ are added as well;

$$T(\cdot, 0) = T_A \quad \text{and} \quad T = T_A \ \text{ on } \partial\Omega. \tag{4}$$

In tumor treatment, the values of the absorption, heat conductivity, pressure density and perfusion, that is, α, κ, ρ and β are usually unknown. These parameters are typically piecewise constants dependent on variations between air, skin, tissue, blood and tumor. The main goal of this work is to estimate these parameters given data, measured by the MRI, on temperature T.

The *ultrasound is crucial here* since variations in temperature are important in the identification of the unknown parameters. These ultrasound excitations cause temperature changes of 3-5 degrees C. In our lab temperature can be measured on a grid with 0.5 mm subinterval widths (assuming the area being treated is roughly 10 mm) and a 5 second time step. We believe it may also be possible to read pressures using techniques discussed in [GFMME] or [LPADSSMBFT]. Of course, if both temperature and pressure readings are desired, the measurements will lie on coarser grids.

The most recent and related work, that we are currently aware of, is [HHMK]. In this paper only temperature readings are available as data and they assume that α and ρ are known. Their analysis area is is segmented into three zones so, overall, there are six unknowns constants.

2. Focusing in Helmholtz Model:

The Helmholtz partial differential equation is used in [HHMK] to model the acoustic pressure waves from an HIFU transducer:

$$\nabla \cdot \left(\frac{1}{\rho}\nabla p\right) + \frac{k^2}{\rho} p = 0 \qquad \text{in } \Omega. \tag{5}$$

Here $k = 2\pi f/c + i\alpha$, ρ is a positive density function, $\alpha \geq 0$ is an absorption coefficient, $c > 0$ is speed of sound and f is frequency of the wave field. We append boundary conditions

$$\frac{\partial p}{\partial \nu} = i2\pi f \rho v \ \text{ on } \Gamma_U \quad \text{and} \quad \frac{\partial p}{\partial \nu} = 0 \ \text{ on } \partial\Omega - \Gamma_U. \tag{6}$$

The velocity v is provided by the ultrasound transducer on boundary portion Γ_U. In [HHMK], the transducer is pulsed and, given an array of transducers may have many v values.

To simplify and make some first steps toward understanding the *focussing* that tends to occur in homogeneous media we assume that ρ is constant, let $\omega = 2\pi f$, require $\alpha = 0$ and assume the problem is posed on a disk with angular symmetry and radius R, so (5) becomes, find $p = p(r)$ for $r \in [0, R]$ so

$$r^2 p'' + r p' + k^2 r^2 p = 0 \quad \text{with} \quad p'(R) = i\rho v k \qquad (k = \frac{\omega}{c})$$

and we assume $\lim_{r\to 0}(rp'(r)) = 0$ as a disc center condition. This will have a Bessel function solution; to derive this, we change variables. Let

$$r = x/k \qquad \text{and} \qquad P(x) = p(x/k) \qquad (\text{So } p(r) = P(kr))$$

and find

$$x^2P'' + xP' + x^2P = 0 \qquad \text{and} \qquad P'(kR) = ic\rho v$$

It is well known (See, for instance, [BC]) that the solution to the differential equation is

$$P(x) = AJ_0(x) + BY_0(x).$$

But, since, $Y_0 \to \pm\infty$ as $x \to 0$ we typically take $B = 0$. Also, since it is known that $J_0' = -J_1$ and thus we can determine a formula for A;

$$-AJ_1(kR) = ic\rho v \qquad => \qquad A = -\frac{ic\rho v}{J_1(kR)}.$$

So,

$$P(x) = -\frac{ic\rho v}{J_1(kR)}J_0(x) \qquad => \qquad p(r) = -\frac{ic\rho v}{J_1(kR)}J_0(kr)$$

From the identity (Again, see [BC])

$$J_1(z) = \frac{2}{\pi}\int_0^{\pi/2} \sin(z\,\sin(\phi))\,\sin(\phi)\,d\phi$$

I believe we can make a reasonable argument that $J_1(kR) \sim 1/k$ for k large (I'm getting abit on a limb with this one ...) and thus have $|A| \sim vk$. From the picture below, we now would have that, at the center of the disc, we get the focussed pressure wave,

$$p(0) \sim kvJ_0(0) = kv.$$

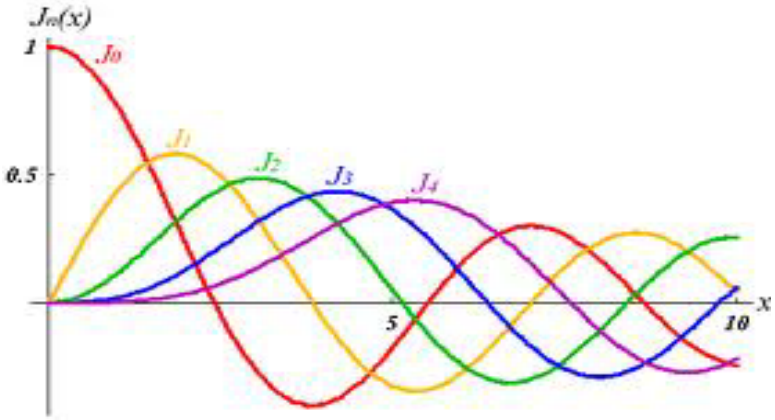

Figure 1: Plot of first few Bessel Functions $J_n(z)$.

Next Steps: Here are some ideas on how to proceed from here on:

- Clearly some follow-thru is needed. Short computations with this Bessel solution would add alot to this little write-up.
- There is a difficulty in the cases when $J_1(kR) = 0$ do not allow a solution to the problem. Probably insisting that $\alpha > 0$ will remedy this but the analysis needs to be done. Perhaps α is small enough, after nondimensionalization, to develop a perturbation solution using the Bessel solution above.

3. Inverse Problem:

The computation of various constant or function coefficients in ordinary or partial differential equation problems is commonly referred to as an inverse problem. Since the terms involving the unknowns often do not "coerce" the coefficient being sought, the task of determining it is ill-posed. This instability may manifest itself as non-uniqueness or extreme sensitivity to noise/errors in the given data.

There are many approaches to solving inverse problems. The book [G] gives an overview of many of the issues. The paper [T] gives one example of an "ad hoc" technique to solve an inverse problem while [EKN] and [EZ] provide an analysis of the standard linearization approach. The paper [Mu] provides an entirely different algorithm.

We hope to use the ideas in [EKN] and [EZ] or [Mu] and [T] to develop a theoretical analysis for a technique that is different from the Bayesian approach in [HHMK].

It seems reasonable to consider a one-dimensional situation (Proof of concept) at first. We should aim to develop both a computer solution and theory about the problem. In one-dimension, if α and ρ are assumed piecewise constant, as in [HHMK], then a solution formula for $p = p(x)$ seems possible The problem defined by (5) and (6) is primarily steady state. However, since the v_n may depend on t, apparently they "pulse" the ultrasound, the solution p, in fact, could change its steady profile from pulse to pulse.

We think it is of value to investigate the qualitative solution behavior using either numerics or closed form solutions probably assuming that β, κ, α and ρ are constant, or at best, piecewise constant. From this we will have a clearer notion of solution behavior and dynamics.

One-Dimensional Elliptic Problem with Piecewise Constant Parameter: We develop and analyze a method for the following inverse problem: Find function $\beta = \beta(x)$ that satisfies the boundary value problem (BVP)

$$-U'' + \beta U = f \quad \text{with boundary conditions} \quad U(0) = U(1) = 0.$$

Suppose there is a piecewise linear data function U_D defined on a partition of $\Omega = [0, 1]$ with subintervals of uniform width h_D and that there is a true solution of the BVP $U = U(x)$ associated with this β. We will assume that the data is close to the true solution; there exists $0 < \epsilon << 1$ so that

$$\|U - U_D\| \leq \epsilon. \tag{7}$$

We further assume that

$$\beta(x) = \begin{cases} \beta_0 \text{ for } 0 \leq x \leq m, \\ \beta_1 \text{ for } m < x \leq 1, \end{cases} \qquad 0 < m < 1.$$

We create smooth cutoff functions $\omega_0 \in C_0^\infty(0, m)$ and $\omega_1 \in C_0^\infty(m, 1)$. It is reasonable to require that derivatives of the ω_i's are $O(1)$ since they "live" on $O(1)$ intervals. We compute an approximation β^A using integration-by-parts twice, the fact that ω_0 and ω_1 are smooth and have support inside $[0, m]$ and $[m, 1]$, respectively, leads to

$$\beta_0^A = \frac{\int_\Omega f\omega_0 \, dx + \int_\Omega U_D\omega_0'' \, dx}{\int_\Omega U_D\omega_0 \, dx} \quad \text{and} \quad \beta_1^A = \frac{\int_\Omega f\omega_1 \, dx + \int_\Omega U_D\omega_1'' \, dx}{\int_\Omega U_D\omega_1 \, dx}.$$

We now will find error bounds for the quantities $|\beta_0 - \beta_0^A|$ and $|\beta_1 - \beta_1^A|$ in terms of h_D and ϵ. It will be necessary to require that there exist positive constants ρ_0 and ρ_1 so that

$$|\int_\Omega U\omega_0 \, dx| \geq \rho_0 > 0 \quad \text{and} \quad |\int_\Omega U\omega_1 \, dx| \geq \rho_1 > 0.$$

We are pursuing an *a priori* style result and so, we will, implicitly assume that norms of U and f as well as bounds of β_0 and β_1 are all $O(1)$.

Lemma 1: There exists a constant C independent of ϵ and h_D such that

$$|\int_\Omega U_D\omega_0 \, dx| \geq \rho_0 - C\epsilon \quad \text{and} \quad |\int_\Omega U_D\omega_1 \, dx| \geq \rho_1 - C\epsilon.$$

Proof: Use true solution U as an intermediate function;

$$\rho_0 \leq |\int_\Omega U\omega_0 \, dx| \leq |\int_\Omega (U - U_D)\omega_0 \, dx| + |\int_\Omega U_D\omega_0 \, dx|$$

Now, using the estimate 7 we can finish the proof for the $0th$ term. The estimate for the other is similar. ///

Thus, lemma 1 guarantees that β_0^A and β_1^A can be computed since the denominators in their definitions cannot be zero.

Theorem: There exists a constant C independent of ϵ and h_D such that

$$\max\{|\beta_0 - \beta_0^A|, |\beta_1 - \beta_1^A|\} \leq C\epsilon.$$

Proof: We show this just for the 0th components. The other term is similar. We start by subtracting the key integrated equations for u_S and U that arose from their respective definitions;

$$(\int_\Omega U_D\omega_0 \, dx) \, \beta_0^A - (\int_\Omega U\omega_0 \, dx) \, \beta_0 = \int_\Omega (U_D - U)\omega_0'' \, dx$$

or

$$(\int_\Omega U_D\omega_0 \, dx)(\beta_0^A - \beta_0) = \int_\Omega (U_D - U)\omega_0'' \, dx + \int_\Omega (U_D - U)\omega_0 \, dx\beta_0.$$

We can now finish our proof using our previous lemma and assumption that we are pursuing an *a priori* style analysis. ///

Kristen's Multi-Parameter Study: The above has been extended to the inverse problem below where the unknown parameters κ and β are sought in the BVP

$$-\kappa U'' + \beta U = f \qquad \text{with} \quad U(0) = U(1) = 0$$

given $f = f(x)$ and data for $U \cong U_D$ where $\beta = O(1000)$ and $\kappa = O(1)$. Both a theoretical analysis and computations with finite difference schemes has been done to show the veracity of the approach.

The difference in sizes for κ and β can lead to subtractive cancellation issues (due to data approximation errors (not floating point)) in the case when U and U'' are $O(1)$ and f is $O(\beta)$. To be more precise, our direct residual technique involves creating equations for the parameters by multiplying the DE by functions ω and integrating by parts over $\Omega = [0, 1]$;

$$\kappa = \frac{\int_\Omega f\omega \, dx - \beta \int_\Omega U\omega \, dx}{\int_\Omega U\omega'' \, dx}$$

So, specifically, the subtractive cancellation arises from the difference calculation of the two large but close (in value) terms in the numerator. Choosing

$$\omega(x) = \epsilon(1 - e^{-x/\epsilon})(1 - e^{-(1-x)/\epsilon})$$

$(0 < \epsilon << 1)$ could help since

$$\int_\Omega U\omega \, dx = O(\epsilon), \quad \int_\Omega f\omega \, dx = O(\beta\epsilon) \quad \text{and} \quad \int_\Omega U''\omega \, dx = \int_\Omega U\omega'' \, dx = O(1)$$

so the calculation of β involves the subtraction of smaller numbers. If this is unsuccessful the other possibility is to investigate modifying f so that the second derivative term is large by itself.

Another alternative would involve approximating the difference with the $O(\beta)$ terms leading to κ considerably more accurately.

Full Parameter Set Study on Reduced Dimension Problem: The next step would be to add the Helmholtz equation and study the inverse problems with unknown parameters α, β, κ and ρ. The most interesting, and, perhaps realistic version, would only assume there was data for the temperature. The two equations are connected thru the source term which may lead to further ill-posedness (see page 64-65 in [G]). This analysis/development would involve incrementally more complicated problems, probably starting with constant coefficients and using known solutions (Mainly for Helmholtz) to finite difference schemes with meshes that fit the piecewise constant partitions exactly – but modest frequencies to, finally, more realistic versions using the enrichment techniques described in section 4.

4. Helmholtz Equation – High Frequencies and Rough Coefficients:

As in [HHMK] we use the Helmholtz equation to model the pressure instead of the KZK [HMB], full second-order wave [SZJ], Burgers or Westervelt equations. (Investigation of these other models in this MRI/HIFU context might provide a new research direction.).

Challenges & Existing Techniques: There are several major challenges associated with solving the Helmholtz equation in the HIFU context. The second order term "competes" with the reaction term making standard stability/energy analyses more difficult. The absorption term ($\alpha > 0$) alleviates this to some extent. At the same time, the transducers are operated in at high frequencies; for accurate resolution in finite difference or element approaches, very fine mesh refinements are required (See [IH1] and [IH2] for more on these challenges).

The relatively current work [MW] uses a Treffitz type method. A discontinuous finite element-type space is developed using known solutions to the Helmholtz equation on each element domain – triangles usually – in a least squares variational form. This strategy is used in [HHMK]; the meshes are fitted to the different large subdomains (Skin, tissue, tumor and air). Thus, on each subdomain a constant coefficient Helmholtz equation is being solved.

Enrichment with XFEM and/or Pseudo-Derivative Mesh Free Schemes: Imbedding appropriate singular functions into approximation spaces is a common idea that we will examine to handle both the material discontinuity and high frequency challenges (Although the approach in [MW] handles this via the introduction of Helmholtz solutions directly into the local element functions). We are interested in XFEM (see [GWB], [SVC] or [VSC]) as well as meshfree (see [BM], [FO], [KLYBL] or [LY]) approaches.

5. Other Directions:

Below are a few other research paths we have pondered.

Nonlinear Inverse Problem: We might extend the current work by looking for conductivity and perfusion as functions of temperature; that is, $\kappa = \kappa(T)$ and $\beta = \beta(T)$. (The use of Gröbner bases may be relevant, hard/interesting? Need to look into work by Marisa Eisenberg, Hans Othmer and Brandy Stigler.).

Optimization of Tranducer Waves: The authors of [HHMK] are interested in the transducer array operation. They provide an optimization algorithm that seeks to arrange the ultrasound sources to provide focused heating but, at the same time, avoid overheating – to minimize tissue damage.

Sensitivity: We will eventually need to estimate sensitivities – either theoretically or computationally. If κ is an unknown then we would be trying to find $\partial\kappa/\partial U_D$.

References

[BM] I. Babuska and J.M. Melenik, The partition of unity method, *Int. J. Num. Meth. Engrg.*, **40** (1997), 727-758.

[BJ] L. Belina and C. Johnson, A posteriori error estimation in computational inverse scattering, *Math. Models Methods Appl. Sci*, **15** (2005), 23-35.

[BC] J.W. Brown and R.V. Churchill, Fourier Series and BVP, McGraw-Hill (5th Edition) (1993).

[EKN] H.W. Engl, K. Kunisch and A. Neubauer, Convergence rates for Tikhonov regularization of nonlinear ill-posed problems, *Inverse Problems*, **5** (1989), 523-540.

[EZ] H.W. Engl and J. Zou, A new approach to convergence rate analysis of Tikhonov regularization for parameter identification in heat conduction, *Inverse Problems*, **16** (2000), 1907-1923.

[FO] D.A. French and M. Osorio, Error estimates for an element free Galerkin method with diffuse derivatives and penalty stabilization, *Computational Mechanics*, **50** (2012), 657-664.

[GFMME] K.J. Glaser, J.P. Felmlee, A. Manduca, Y.K. Mariappan and R.L. Ehman, Stiffness-weighted magnetic resonance imaging, *Magnetic Resonance in Medicine*, **55** (2006), 59-67.

[G] C. W. Groetsch, *Inverse Problems in the Mathematical Sciences*, Vieweg (1993).

[GWB] R. Gracie, H. Wang and T. Belytschko, Blending in the extended finite element method by discontinuous Galerkin and assumed strain methods, *Int. J. Num. Meth. Engrg.*, **74** (2008), 1645-1669.

[HC] G.T. Haar and C. Coussios, High intensity focused ultrasound: physical principles and devices, *Int. J. Hyperthermia*, **23** (2007), 89-104.

[HHMK] J.M.J. Huttunen, T. Huttunen, M. Malinen and J.P. Kaipio, Determination of heterogeneous thermal parameters using ultrasound induced heating and MR thermal mapping, *Phys. Med. Biol.*, **51** (2006), 1011-1032.

[HMB] P. Hariharan, M.R. Myers and R.K. Banerjee, HIFU procedures at moderate intensities – effect of large blood vessels, *Phys. Med. Biol.*, **52** (2007), 3493-3513.

[IH1] F. Ihlenburg and I. Babuska, Finite element solution of the Helmholtz equation with high wave number. Part I: The h-version of the FEM, *Comp. Math. Appl.*, **30** (1995), 9-37.

[IH2] F. Ihlenburg and I. Babuska, Solution of Helmholtz problems by knowledge-based FEM, *Comp. Assisted Mech. Engrg. Sci.*, **4** (1997), 397-415.

[JM] B. Jin and L. Marin, The method of fundamental solutions for inverse problems associated with the steady-state heat conduction, *Internat. J. Numer. Methods Engrg.*, **69** (2007), 1570-1589.

[KLYBL] D. W. Kim, W.K. Liu, Y.-C. Yoon, T. Belytschko and S.-H. Lee, Meshfree point collocation method with intrinsic enrichment for interface problems, *Comput. Mech.*, **40** (2007), 1037-1052.

Table 1: Model Data – Parameters and Definitions from [HHMK] and [HMB]:

Label	**Name**	**Value**
c	Speed of Sound	1560 ms^{-1}
C_B	Heat Capacity of Blood	3770 $J\ kg^{-1}\ K^{-1}$
ρ	Tissue Density	1000 $kg\ m^{-3}$
α	Absorption Coefficient	1 $dB/(MHz\ cm)$
L	Length scale	30 cm
C_T	Specific Heat	3770 $J\ kg^{-1}\ K^{-1}$
T_A	Arterial Blood Temperature	300 K
ω_B	Blood Density	1000 $kg\ m^{-3}$
f	Frequency of Ultrasound Inducers	500 kHz
κ	Tissue Thermal Conductivity	0.6 $W\ K^{-1}\ m^{-1}$
v_n	Transducer Velocity	1000 ms^{-1}

[LPADSSMBFT] B. Larrat, M. Pernot, J.F. Aubry, E. Dervishi, R. Sinkus, D. Seilhean, and Y. Marie, A.L. Boch, M. Fink and M. Tanter, MR-guided transcranial brain HIFU in small animal models, *Phys. Med. Biol.*, **55** (2010), 365-388.

[LY] S.-H. Lee and Y.-C. Yoon, Enriched meshfree collocation method with diffuse derivatives for elastic fracture, *Int. J. Num. Meth. Engrg.*, **61** (2004), 22-48.

[MW] P. Monk and D.-Q. Wang, A least squares method for the Helmholtz equation, *Comp. Meth. Appl. Mech. Engrg.*, **175** (1999), 121-136.

[Mu] D.A. Murio, The mollification method and the numerical solution of the inverse heat conduction problem by finite differences, *Computers Math. Applic.*, **17** (1989), 1385-1396.

[SZJ] W. Sun, M. Zhang and X. Juan, The simulation of temperature field for HIFU phased array transducer, *IEEE Explore*, 6 pages.

[T] M. Tadi, Inverse heat conduction based on boundary measurement, *Inverse Problems*, **13** (1997), 1585-1605.

[SVC] B. G. Smith, B. L. Vaughan, & D. L. Chopp. The Extended Finite Element Method for Boundary Layer Problems in Biofilm Growth. *CAMCoS*, **2** (2007), 35-56.

[VSC] B.L. Vaughan, B.G. Smith and D.L. Chopp, A comparison of the XFEM with IBM for elliptic equations with discontinuous coefficients and singular sources, *Comm. App. Math. Comp. Sci.*, **1** (2006), 207-228.

Table 2 – Estimates of Parameters from [HHMK] (Page 1020):

Material	$\alpha\ (dB/(MHz\,cm))$	$c\ (ms^{-1})$	$\rho\ \ (kg\,m^{-3})$	$\kappa\ \ (WK^{-1}m^{-1})$	$C_T\ \ (J\,kg^{-1}K^{-1})$	$\omega_B\ \ (kg\,m^{-3}s^{-1})$
Air	0	1500	1000	0.60	4190	0
Skin	12	1610	1200	0.50	3770	1.0
Tissue	5	1485	1020	0.50	3550	0.7
Tumor	5	1547	1050	0.65	3770	2.3

Appendix I – Solutions to the Linear Pressure Equation.

If we consider the special case where density ρ is identically equal to 1 in one-dimension on $[0, L]$ we can make a beginning assessment of the form of the solution $p(x)$. Here we wish to solve

$$p'' + k^2 p = 0 \qquad p'(0) = iP_0 \qquad (k = f + i\alpha,\ \alpha > 0.)$$

If the boundary condition at the right "end" point is either absorbing as in [HHMK],

$$p'(L) - ikp(L) = 0$$

or requires $p \to 0$ as $x \to \infty$, then we have

$$p(x) = Ae^{ifx}e^{-\alpha x} \qquad \text{or} \qquad p(x) = \frac{P_0 e^{ifx}e^{-\alpha x}}{f + i\alpha}.$$

Note, in particular, in this case the high frequency oscillation is not present in the heat source term $Q = Q(x)$ since the absolute value of pressure becomes:

$$|p(x)| = \frac{P_0 e^{-\alpha x}}{\sqrt{f^2 + \alpha^2}}.$$

We can then choose $P_0 = A_0 f e^{\alpha x}$ so

$$|p(x)| = A_0 \left(\frac{f}{\sqrt{f^2 + \alpha^2}} \right) e^{-\alpha(x - x_0)}.$$

If, instead, we impose $p'(L) = 0$ at the right end point we find

$$p(x) = \frac{iP_0 \cos(k(x-L))}{k \sin(kL)}$$

and

$$|p(x)| = \frac{P_0}{\sqrt{f^2+\alpha^2}} \sqrt{\frac{\cos(2fx)+\cosh(2\alpha x)}{\cos(2fL)-\cosh(2\alpha L)}}.$$

MR-Guided HIFU System:

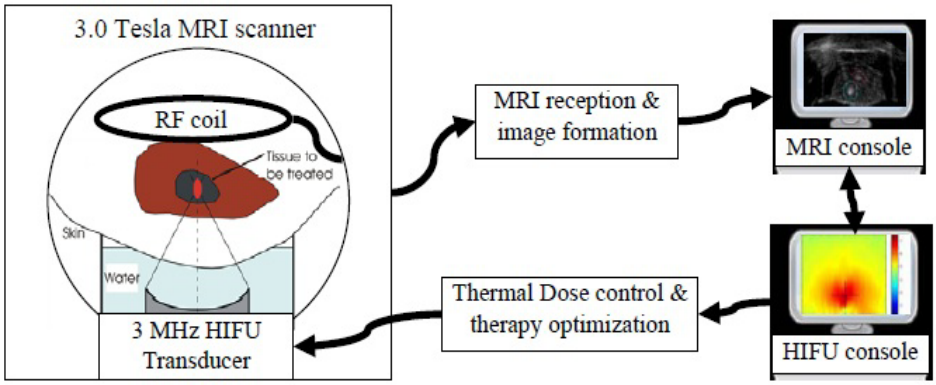

Figure 2: A feedback control system for preclinical thermal therapy was established using MRguided HIFU in the CCHMC IRC. The feedback control loop is formed using a 3.0 Tesla 32-channel Philips Achieva MR scanner (Philips HealthCare, Best, the Netherlands) and a Philips small-animal HIFU system (Philips HealthCare, Vantaa, Finland). The current system uses a single channel RF coil for animal imaging and an eight-channel 3 MHz sectored transducer (IMASONIC, Voray sur I'Ognon, France) for acoustic transmission. The development of a multichannel RF coil array for high-speed MR imaging of mice is ongoing.